

On the necessity of a consistent likelihood-based approach to model magnitude dispersion in type Ia supernovae observations

B. L. Lago,^{a,c} M. O. Calvão,^a S. E. Jorás,^a R. R. R. Reis,^a I. Waga^a
and R. Giotri^b

^aInstituto de Física, Universidade Federal do Rio de Janeiro
C. P. 68528, CEP 21941-972, Rio de Janeiro, RJ, Brazil

^bDepartamento de Engenharia Rural
Universidade Federal do Espírito Santo
C. P. 16, CEP 29500-000, Alegre, ES, Brazil

^cCoordenação de Licenciatura em Física, Centro Federal de Educação Tecnológica Celso
Suckow da Fonseca, CEP 28635-000, Nova Friburgo, RJ, Brazil

E-mail: brunolz@if.ufrj.br, orca@if.ufrj.br, joras@if.ufrj.br, ribamar@if.ufrj.br,
ioav@if.ufrj.br, rgiotri@if.ufrj.br

Abstract. In this article we present an alternative, numerically efficient, statistical analysis of type Ia supernovae (SNe Ia) data: instead of performing the traditional χ^2 procedure, we suggest working with the complete likelihood itself. Indeed the latter must be used instead of the former when dealing with parameters in the expression for the variance — which is exactly the case of SNe Ia surveys, using either MLCS2k2 or SALT2 light-curve fitters. Although these two analyses are in principle distinct, we find no significant quantitative differences, for cosmological parameters, in either best fits or confidence intervals estimation when using current SNe Ia data. We conjecture that this practical equivalence may not remain when dealing with future SNe Ia data.

Keywords: supernova type Ia – standard candles, dark energy experiments, dark energy theory

ArXiv ePrint: [1104.2874](https://arxiv.org/abs/1104.2874)

Contents

1	Introduction	1
2	Light-curve fitting	2
3	The traditional χ^2 analysis	4
3.1	The χ^2 analysis from SALT2 output	4
3.2	The χ^2 analysis from MLCS2k2 output	6
4	The proposed likelihood analysis	6
5	Results	7
5.1	Comparison of constraints	7
5.2	Comparison of model selection	9
5.3	Investigating evolution of the SALT2 parameters α , β , \mathcal{M} and σ_{int} with redshift	12
6	Conclusions	12

1 Introduction

By the end of the last century observations of type Ia supernovae (SNe Ia), used as standard candles, directly established the acceleration of the universe [1, 2], an awesome result, possibly only surpassed by the discovery of its very own expansion, around eighty years ago [3]. They are still the backbone for the prevailing Λ CDM concordance model, which is furthermore corroborated by the combination of other probes, such as, e.g., cosmic microwave background anisotropies [4], baryon acoustic oscillations [5, 6] and galaxy clustering [7, 8].

The sample standard deviation in the inferred, uncorrected absolute B magnitude of typical sets of SNe Ia is of the order 0.4 (even after the exclusion of outliers such as the overluminous 1991T-like SNe Ia and the underluminous 1991bg-like SNe Ia) [9–12]. This amounts to a fractional uncertainty in luminosity of -30% and (under the assumption of negligible uncertainties in all other quantities) in luminosity distance of 20% . It is thus clear that SNe Ia are not exactly *prima facie* standard candles at all. However, even such a scatter, as compared to other categories of astrophysical sources (other supernova types, gamma-ray bursts, etc), is small and, in conjunction with their typical high peak luminosity (10^{36} W $\sim 4 \times 10^9 L_{\odot}$), justifies the effort to improve their use as cosmological *standardizable* candles. After the standardization recipe (cf. Section 2), the scatter in M_B decreases to around 0.15, which amounts to a fractional uncertainty in luminosity of -13% and in luminosity distance of 7% .

Already in the landmark papers from the two original surveying groups [1, 2], a legitimate concern was expressed about the presence of not properly accounted for systematic effects. At that time, however, there was only a small number (the order of tens) of observed SNe Ia in any of the available samples, so the uncertainties were statistically limited; the main task was gathering new, larger, uniform datasets. For the recent compilations and surveys [13–18], and the more so for the future ones [19–21], we are no longer sample-limited; the urgency is again on the physics of the SN Ia phenomenon and all the aspects which

impact it: nature of progenitor binary system (single-degenerate versus double degenerate, tardy versus prompt events) [22–24], properties of host galaxy [25, 26], mechanisms of explosion [27], extinction/intrinsic color variations [28, 29], K-correction and template calibration [30, 31], flux calibration [32], inhomogeneities (peculiar velocities [33, 34], gravitational lensing [35, 36], etc). We would also like to call attention to the particularly clear, informative and up-to-date generic review articles on SNe Ia by Howell [37], Kirshner [38], and Goobar & Leibundgut [39]. Simultaneously with this physical endeavor from first principles, we should also exercise our best statistical consistent practices to analyze and mine the data and to test the robustness of our inferences. It is to this last task that our paper is devoted.

Our aim is twofold. First of all, and most importantly, we present a statistically self-consistent, well-grounded and numerically efficient approach to both parameter fitting and model selection, based on the likelihood, in contrast to the traditional χ^2 analysis present in most of the literature. More concretely, we call attention to the simple fact that, when we want to estimate both the covariance and the mean of a Gaussian process, the ordinary (uncorrected) χ^2 analysis (or any iterative recipe therefrom, for that matter) cannot be straightforwardly applied, lest we might lose a nontrivial term in the objective function to be extremized. This is particularly worrisome when the covariance itself does depend on free parameters of the underlying model. The analysis we advocate in the present work is neither new in the statistical literature nor numerically less efficient than the traditional recipes and it is easily generalized to the aforementioned situation. As a matter of principle, the analyses yield distinct results, which takes us to our second goal: We compare the quantitative results of previous real-data treatments and the present one. In particular, we point out that future surveys may lead to different conclusions depending on the chosen approach.

Here we restrict ourselves to SNe Ia real, observed, datasets only, without taking into account other important sources of information (such as CMB, BAOs or clusters) in order to make our point pristine, by avoiding the masking due to any other such probes.

The structure of the paper is as follows. In Section 2, we briefly remind the general procedure to go from the raw data to the final estimated parameters. In Section 3, we describe the two most widely used “fitter pipelines” (MLCS2k2 and SALT2), which use the traditional χ^2 analysis. In Section 4, we criticize the aforementioned usual approaches and present the new likelihood-based one. In Section 5, the main numerical results are shown, for both fitters and several datasets. Finally, in Section 6, we end up with some discussions and conclusions.

2 Light-curve fitting

The “primary” data of any SN Ia survey are apparent magnitudes (or fluxes) in a given set of filters, at a series of epochs (phases), for each supernova. This constitutes an array $m_{i,Y,\alpha}$ ($f_{i,Y,\alpha}$), where i labels the supernova, Y labels the filter (or band) and α labels the epoch in the time series. For a given supernova i , observed in a given filter Y , the scatterplot of the points $(t_\alpha, m_{i,Y,\alpha})$, where t_α is the observed time, is what we call (a sampling of) the raw light curve.

As mentioned in Section 1, SNe Ia are *standardizable* candles; this means there is a phenomenological recipe whereby the raw light curves, after being subjected to a transformation by a N_{st} -parameter function, furnish a new set of so-called *standardized* light curves; this means the dispersion in the new magnitudes is considerably smaller than in the original input set. The aforementioned phenomenological recipe is not unique at all: there are several

light-curve fitters in the literature [40–57]. Here we will exploit some features of the two most common ones: the Multicolor Light-Curve Shape (MLCS) [1, 40, 41, 58] one and the Spectral Adaptive Light curve Template (SALT) [52, 53].

In a nutshell, in their most recent incarnations:

- The MLCS2k2 fitting model [41] describes the variation among SNe Ia light curves with a single parameter (Δ). Excess color variations relative to the one-parameter model are assumed to be the result of extinction by dust in the host galaxy and in the Milky Way. The MLCS2k2 model magnitude, observed in an arbitrary filter Y , at an epoch α , is given by

$$m_{Y,\alpha}^{\text{model}} = M_{Y',\alpha} + p_{Y',\alpha}\Delta + q_{Y',\alpha}\Delta^2 + K_{Y'Y,\alpha} + \mu + X_{Y',\alpha}^{\text{host}} + X_{Y,\alpha}^{\text{MW}}, \quad (2.1)$$

where $Y' \in \{U, B, V, R, I\}$ is one of the supernova rest-frame filters for which the model is defined, Δ is the MLCS2k2 shape-luminosity parameter that accounts for the correlation between peak luminosity and the shape/duration of the light curve. Furthermore, the model for the host-galaxy extinction is $X_{Y',\alpha}^{\text{host}} = \zeta_{Y',\alpha}(a_{Y'} + b_{Y'}/R_V)A_V$, where $\zeta_{Y',\alpha} := X_{Y',\alpha}^{\text{host}}/X_{Y',0}^{\text{host}}$, and $a_{Y'}$, $b_{Y'}$ are constants; as usual, A_V is the V band extinction, at B band peak ($a_V = 1$, $b_V = 0$), and $R_V := A_V/E(B - V)$, the ratio of V band extinction to color excess, at B band peak. Finally, $X_{Y,\alpha}^{\text{MW}}$ is the Milky Way extinction, $K_{Y'Y,\alpha}$ is the K -correction between rest-frame and observer-frame filters, and μ is the distance modulus. The coefficients $M_{Y',\alpha}$, $p_{Y',\alpha}$, and $q_{Y',\alpha}$ are model vectors that have been evaluated using nearly 100 well observed low-redshift SNe Ia as a training set. $\alpha = 0$ is the B band peak magnitude epoch.

Fitting the model to each SN Ia magnitudes, usually fixing R_V gives μ , Δ , A_V and t_0 , the B -band peak magnitude epoch.

- The SALT2 fitter [53] relies on a two-dimensional surface in time and wavelength that describes the temporal evolution of the rest-frame spectral energy distribution (SED) for SNe Ia. The model is created from a combination of photometric light curves and hundreds of SNe Ia spectra.

In SALT2, the rest-frame flux at wavelength λ and time t ($t = 0$ at B -band maximum) is modeled by

$$\frac{dF_{rest}}{d\lambda}(t, \lambda) = x_0[M_0(t, \lambda) + x_1M_1(t, \lambda)] \exp[cC(\lambda)]. \quad (2.2)$$

$M_0(t, \lambda)$, $M_1(t, \lambda)$, and $C(\lambda)$ are determined from the training process described in [53]. $M_0(t, \lambda)$, $M_1(t, \lambda)$ are the zeroth and the first moments of the distribution of training sample SEDs. One might consider adding moments of higher order to Eq. (2.2).

To compare with photometric SNe Ia data, the observer frame flux in passband Y is calculated as

$$F_{obs}^Y = (1 + z) \int d\lambda' \left[\lambda' \frac{dF_{rest}}{d\lambda'}(t, \lambda') T^Y(\lambda'/(1 + z)) \right], \quad (2.3)$$

where $T^Y(\lambda)$ defines the transmission curve of the observer-frame filter Y , and z is the redshift.

Each SN Ia light curve is fitted separately using Eqs. (2.2) and (2.3) to determine the parameters x_0 , x_1 , and c . However, the SALT2 light-curve fit does not yield an independent distance modulus estimate for each SN Ia. As we will see in the next section, the distance moduli are determined as part of a global parameter fit to an ensemble of SN Ia light curves in which cosmological parameters and global SN Ia properties are also determined.

In the next section we will discuss how to obtain constraints on cosmological parameters using MLCS2k2 and SALT2 output quantities as our data.

3 The traditional χ^2 analysis

The prevailing SNe Ia cosmological analysis is based on the χ^2 function:

$$\chi^2 := \mathbf{X}^T \boldsymbol{\Sigma}^{-1} \mathbf{X} \quad (3.1)$$

where $\mathbf{X} := (\boldsymbol{\mu} - \boldsymbol{\mu}_{th}(\mathbf{z}, \boldsymbol{\Theta}))$, $\boldsymbol{\mu}$ is the set of distance moduli derived from the light curve fitting procedure for each SN Ia event, at redshifts given by \mathbf{z} , $\boldsymbol{\mu}_{th}(\mathbf{z}, \boldsymbol{\Theta})$ is the theoretical prediction for them, given in terms of a vector $\boldsymbol{\Theta}$ of parameters and $\boldsymbol{\Sigma}$ is the covariance matrix of the events.

As discussed in the previous section, each light curve fitter gives a different set of output or processed data, which are not related to the distance modulus in the same way. In this work, to construct the traditional χ^2 function of this section or the proposed likelihood function of the next section, we consider as “data” the distance modulus estimation obtained from MLCS2k2 and SALT2 processing.

3.1 The χ^2 analysis from SALT2 output

The SALT2 light curve fitter gives three quantities, with corresponding errors, to be used in the analysis of cosmology: $m_B^* = -2.5 \log[x_0 \int d\lambda' M_0(t=0, \lambda') T^B(\lambda')]$, the peak rest-frame magnitude in the B band, x_1 , a parameter related to the stretch of the light-curve and c , related to the color of the supernova alongside the redshift z of the supernova. We can derive the distance modulus from these quantities introducing two new parameters, $\boldsymbol{\delta} := (\alpha, \beta)$, plus the peak absolute magnitude, in B band, M_B . Defining the corrected magnitude as

$$m_B^{\text{corr}}(\boldsymbol{\delta}) := m_B^* + \alpha x_1 - \beta c \quad (3.2)$$

we can write

$$\mu(\boldsymbol{\delta}, M_B) = m_B^{\text{corr}}(\boldsymbol{\delta}) - M_B \quad (3.3)$$

Assuming that all SNe Ia events are independent, one can rewrite Eq. (3.1) as

$$\chi_{\text{SALT2}}^2(\boldsymbol{\theta}, \boldsymbol{\delta}, \mathcal{M}(M_B, h)) := \sum_{i=1}^N \frac{[\mu_i(\boldsymbol{\delta}, M_B) - \mu_{th}(z_i; \boldsymbol{\theta}, h)]^2}{\sigma_i^2(\boldsymbol{\delta}) + \sigma_{\text{int}}^2} \quad (3.4)$$

where N is the number of SNe Ia in the sample, $\boldsymbol{\theta}$ denotes the cosmological parameters other than h , with the present value of the Hubble parameter given by $H_0 = 100h \text{ km} \cdot \text{s}^{-1} \cdot \text{Mpc}^{-1}$. Here we have defined

$$\mu_{th}(z; \boldsymbol{\theta}, h) := 5 \log[\mathcal{D}_L(z; \boldsymbol{\theta})] + \mu_0(h). \quad (3.5)$$

with

$$\mu_0(h) := 42.38 - \log h. \quad (3.6)$$

The dimensionless luminosity distance (in units of the Hubble distance today), \mathcal{D}_L , for co-moving observers in a Robertson-Walker universe, is given by

$$\mathcal{D}_L(z; \boldsymbol{\theta}) = \begin{cases} (1+z) \left(\frac{1}{\sqrt{\Omega_{k0}}} \right) \sinh \left(\sqrt{\Omega_{k0}} \int_{z'=0}^z \frac{1}{E(z'; \boldsymbol{\theta})} dz' \right), & \text{if } \Omega_{k0} > 0, \\ (1+z) \int_{z'=0}^z \frac{1}{E(z'; \boldsymbol{\theta})} dz', & \text{if } \Omega_{k0} = 0, \\ (1+z) \left(\frac{1}{\sqrt{-\Omega_{k0}}} \right) \sin \left(\sqrt{-\Omega_{k0}} \int_{z'=0}^z \frac{1}{E(z'; \boldsymbol{\theta})} dz' \right), & \text{if } \Omega_{k0} < 0, \end{cases} \quad (3.7)$$

where Ω_{k0} is the ‘‘curvature density parameter’’ (whatever the underlying dynamical gravitational theory), such that it is proportional to the three-curvature, and

$$E(z; \boldsymbol{\theta}) := H(z; \boldsymbol{\theta}, h) / H_0 \quad (3.8)$$

is the dimensionless Hubble parameter. As indicated in Eq. (3.4), the χ^2 function depends on the parameters M_B and h only through their combination

$$\mathcal{M}(M_B, h) := M_B + \mu_0(h). \quad (3.9)$$

It may thus be thought of as effectively directly dependent on only the parameters $\boldsymbol{\theta}$, $\boldsymbol{\delta}$ and \mathcal{M} .

A floating dispersion term, σ_{int} , ‘‘which contains potential sample-dependent systematic errors that have not been accounted for and the observed intrinsic SNe Ia dispersion’’ [17], is added in quadrature to the distance modulus dispersion, which is given by

$$\sigma_i^2(\boldsymbol{\delta}) = \sigma_{m_B^*, i}^2 + \alpha^2 \sigma_{x_1, i}^2 + \beta^2 \sigma_{c, i}^2 + 2\alpha \sigma_{m_B^*, x_1, i} - 2\beta \sigma_{m_B^*, c, i} - 2\alpha\beta \sigma_{x_1, c, i}. \quad (3.10)$$

We will assume, for simplicity, that the light curve parameters (m_B^*, x_1, c) are uncorrelated and drop the last three terms in Eq. (3.10). This is not the case for the present datasets and any detailed analysis must account for the full covariance of these parameters. Here, we also neglect the contribution for the distance modulus dispersion from redshift measurement uncertainties and peculiar velocities.

As advocated by some groups [59], minimizing Eq. (3.4) gives rise to a bias towards increasing values of α and β . In order to circumvent this feature an iterative method is performed, according to their approach.

In this iterative method, the χ^2 defined in Eq. (3.4) is replaced by

$$\chi_{\text{SALT2}}^2(\boldsymbol{\theta}, \boldsymbol{\delta}, \mathcal{M}) := \sum_{i=1}^N \frac{[\mu_i(\boldsymbol{\delta}, M_B) - \mu_{\text{th}}(\boldsymbol{\theta}, h; z_i)]^2}{\sigma_i^2(\boldsymbol{\eta}) + \sigma_{\text{int}}^2}. \quad (3.11)$$

Notice that, in this expression, $\boldsymbol{\eta}$ is not a parameter of the χ_{SALT2}^2 . In order to obtain the best fit values for the parameters, $\boldsymbol{\eta}$ is given initial values and the optimization is performed on $\boldsymbol{\theta}$, $\boldsymbol{\delta}$ and \mathcal{M} . After this step, $\boldsymbol{\eta}$ is updated with the best fit value of $\boldsymbol{\delta}$ and the optimization is performed again. The process continues until a convergence is achieved, which means that $\boldsymbol{\eta}$ does not change under the required precision.

During this process σ_{int} is not considered as a free parameter to be optimized, being determined rather by the following procedure: Start with a guess value (usually $\sigma_{\text{int}} = 0.15$).

Perform the iterative procedure described above. The value of σ_{int} is then obtained by fine tuning it so that the reduced χ^2 equals unity (with all the other parameters fixed on their best fit values). The iterative procedure is repeated once more with this new value and the final best fit values are obtained. It is important to note that the value of σ_{int} affects both the best fit and the confidence levels of the parameters, since it changes the weight given to each supernova in the χ^2 [cf. Eq. (3.11)].

3.2 The χ^2 analysis from MLCS2k2 output

The MLCS2k2 light curve fitter is also a distance estimator and gives us directly a cosmology-independent estimation of the distance modulus. In this context, the analogue of Eq. (3.4) is

$$\chi_{\text{MLCS2k2}}^2(\boldsymbol{\theta}, h) := \sum_i^N \frac{[\mu_i - \mu_{\text{th}}(\boldsymbol{\theta}, h; z_i)]^2}{\sigma_i^2 + \sigma_{\text{int}}^2} \quad (3.12)$$

where σ_i is the distance modulus dispersion as given by MLCS. We again neglect contributions from redshift measurements and peculiar velocities.

The procedure to obtain σ_{int} is similar to the one described in the previous Subsection, however, in this case we use only a subsample of nearby SNe Ia and not the full one, as for the SALT2 analysis. After setting up the value of σ_{int} , we minimize the χ_{MLCS2k2}^2 using the full SNe Ia sample to obtain the best fit values for $\boldsymbol{\theta}$ and h .

4 The proposed likelihood analysis

Considering the SNe Ia light curve fitting parameters as Gaussian distributed random variables, we propose to take as starting point the likelihood

$$L = \frac{1}{\sqrt{(2\pi)^N \det \boldsymbol{\Sigma}}} \exp(-\mathbf{X}^T \boldsymbol{\Sigma}^{-1} \mathbf{X} / 2), \quad (4.1)$$

which is related to the χ^2 in Eq. (3.1) by

$$\mathcal{L} := -2 \ln L = \chi^2 + \ln \det \boldsymbol{\Sigma} + N \ln(2\pi). \quad (4.2)$$

Eqs. (4.1) and (4.2) are the single basis upon which our whole statistical procedure lies. When the full covariance of the problem is known, minimizing χ^2 is completely equivalent to minimizing \mathcal{L} . However, this is not the case for current SNe Ia observations and neglecting the last but one term in Eq. (4.2) would, in principle, lead to a biased result. Our proposal is minimizing the following functions for each case discussed in the previous section

$$\mathcal{L}_{\text{SALT2}}(\boldsymbol{\theta}, \boldsymbol{\delta}, \mathcal{M}, \sigma_{\text{int}}) = \chi_{\text{SALT2}}^2(\boldsymbol{\theta}, \boldsymbol{\delta}, \mathcal{M}, \sigma_{\text{int}}) + \sum_i^N \ln(\sigma_i^2(\boldsymbol{\delta}) + \sigma_{\text{int}}^2) \quad (4.3)$$

and

$$\mathcal{L}_{\text{MLCS2k2}}(\boldsymbol{\theta}, h, \sigma_{\text{int}}) = \chi_{\text{MLCS2k2}}^2(\boldsymbol{\theta}, h, \sigma_{\text{int}}) + \sum_i^N \ln(\sigma_i^2 + \sigma_{\text{int}}^2), \quad (4.4)$$

where we neglected parameter-independent terms. $\chi_{\text{SALT2}}^2(\boldsymbol{\theta}, \boldsymbol{\delta}, \mathcal{M}, \sigma_{\text{int}})$ and $\chi_{\text{MLCS2k2}}^2(\boldsymbol{\theta}, h, \sigma_{\text{int}})$ are given, respectively, by Eqs. (3.4) and (3.12) now considering σ_{int} *also as a free parameter*. With this procedure, we can obtain directly unbiased probability distributions functions for all parameters, including σ_{int} and $\boldsymbol{\delta}$.

5 Results

In this section we compare the results obtained from the χ^2 and the likelihood analyses, as described in Sections 3 and 4, using real data from the SDSS first year compilation [16], the Union 2 compilation [17] and the SNLS third year compilation [18].

In order to perform the comparison, we considered the following cosmological models:

- Λ CDM, in which we can write the Friedmann equation, in terms of the parameters $\boldsymbol{\theta} = (\Omega_{m0}, \Omega_{k0})$, as

$$E^2(z; \boldsymbol{\theta}) = \Omega_{m0}(1+z)^3 + \Omega_{k0}(1+z)^2 + (1 - \Omega_{m0} - \Omega_{k0}). \quad (5.1)$$

- w CDM, described by $\boldsymbol{\theta} = (\Omega_{m0}, \Omega_{k0}, w)$ and

$$E^2(z; \boldsymbol{\theta}) = \Omega_{m0}(1+z)^3 + \Omega_{k0}(1+z)^2 + (1 - \Omega_{m0} - \Omega_{k0})(1+z)^{3(1+w)}. \quad (5.2)$$

- The Dvali-Gabadadze-Porrati (DGP) brane world model [60], in which $\boldsymbol{\theta} = (\Omega_{m0}, \Omega_{k0})$ and

$$E^2(z; \boldsymbol{\theta}) = \Omega_{k0}(1+z)^2 + (\sqrt{\Omega_{m0}(1+z)^3 + \Omega_{r_c}} + \sqrt{\Omega_{r_c}})^2, \quad (5.3)$$

where $\Omega_{r_c} := 1/(4r_c^2 H_0^2) = (1 - \Omega_{m0} - \Omega_{k0})^2/[4(1 - \Omega_{k0})]$, and r_c is a length scale related to the 5-dimensional Planck mass.

- The quartessence generalized Chaplygin gas (GCG) is described by the equation of state $p = -A/\rho^{\alpha_c}$ [61–64], which leads to

$$E^2(z; \boldsymbol{\theta}) = \Omega_{k0}(1+z)^2 + (1 - \Omega_{k0}) \left[A + (1 - A)(1+z)^{3(1+\alpha_c)} \right]^{1/(1+\alpha_c)}. \quad (5.4)$$

In this model, $\boldsymbol{\theta} = (\Omega_{k0}, A, \alpha_c)$.

5.1 Comparison of constraints

We chose the Λ CDM and Flat w CDM models to directly compare the best-fit and the 68% confidence intervals for the parameters $\boldsymbol{\delta}$, \mathcal{M} , σ_{int} and $\boldsymbol{\theta}$, for SALT2 data, and σ_{int} , $\boldsymbol{\theta}$ and h , for MLCS2k2 data. The fitting is performed with the MIGRAD minimization of the Minuit [65] implementation in ROOT [66]. The results are shown in Tables 1 and 2 for SALT2 and MLCS2k2 data, respectively. It is clear that the best-fit values given for each analysis, although slightly different, have essentially the same confidence intervals.

Since applying both analyses to the data gave essentially the same result for the best-fit values, we investigated, for the SALT2 output, the role played by σ_{int} . We considered a hypothetical situation in which we would have an outstanding control of the systematics such that we could determine σ_{int} prior to the cosmological parameters determination (for the MLCS2k2 data, in this case, the analyses would be equivalent). To that end we fixed its value and performed the optimization, via MCMC, with respect to the other parameters. In Fig. 1 we show the difference between the best-fit values for $\boldsymbol{\theta}$, $\boldsymbol{\delta}$ and \mathcal{M} taken from the likelihood and the χ^2 . The error bars were obtained propagating the 68% confidence intervals from each one. It turned out that for $\sigma_{\text{int}} \lesssim 0.08$ the best-fit values obtained for some parameters, in particular for β , are different at least at the 68% confidence level for all samples.

SALT2

SDSS	ΛCDM	Ω_{m0}	Ω_{k0}	α	β	\mathcal{M}	σ_{int}
	\mathcal{L}	0.282 ± 0.062	0.06 ± 0.18	0.0927 ± 0.0079	2.174 ± 0.073	23.394 ± 0.018	0.1271 ± 0.0074
	χ^2	0.281 ± 0.058	0.07 ± 0.17	0.0913 ± 0.0077	2.131 ± 0.077	23.396 ± 0.018	0.1358 –
	<hr/>						
	FwCDM	Ω_{m0}	w	α	β	\mathcal{M}	σ_{int}
	\mathcal{L}	0.283 ± 0.077	–0.95 ± 0.21	0.0927 ± 0.0079	2.174 ± 0.073	23.394 ± 0.019	0.1271 ± 0.0074
	χ^2	0.281 ± 0.081	–0.94 ± 0.22	0.0912 ± 0.0077	2.132 ± 0.077	23.396 ± 0.020	0.1358 –
Union 2	ΛCDM	Ω_{m0}	Ω_{k0}	α	β	\mathcal{M}	σ_{int}
	\mathcal{L}	0.299 ± 0.055	0.01 ± 0.14	0.1044 ± 0.0049	2.295 ± 0.047	23.262 ± 0.010	0.1231 ± 0.0056
	χ^2	0.301 ± 0.055	0.02 ± 0.14	0.1017 ± 0.0050	2.247 ± 0.045	23.269 ± 0.012	0.1365 –
	<hr/>						
	FwCDM	Ω_{m0}	w	α	β	\mathcal{M}	σ_{int}
	\mathcal{L}	0.288 ± 0.060	–0.96 ± 0.15	0.1044 ± 0.0049	2.294 ± 0.047	23.263 ± 0.012	0.1231 ± 0.0056
	χ^2	0.290 ± 0.064	–0.95 ± 0.16	0.1016 ± 0.0050	2.246 ± 0.045	23.270 ± 0.012	0.1365 –
SNLS	ΛCDM	Ω_{m0}	Ω_{k0}	α	β	\mathcal{M}	σ_{int}
	\mathcal{L}	0.35 ± 0.11	0.03 ± 0.42	0.1141 ± 0.0089	2.569 ± 0.086	23.547 ± 0.068	0.1193 ± 0.0083
	χ^2	0.335 ± 0.053	0.05 ± 0.19	0.1155 ± 0.0089	2.621 ± 0.076	23.542 ± 0.045	0.1167 –
	<hr/>						
	FwCDM	Ω_{m0}	w	α	β	\mathcal{M}	σ_{int}
	\mathcal{L}	0.33 ± 0.14	–0.90 ± 0.48	0.1141 ± 0.0089	2.570 ± 0.086	23.555 ± 0.067	0.1193 ± 0.0082
	χ^2	0.316 ± 0.048	–0.89 ± 0.17	0.1155 ± 0.0089	2.621 ± 0.077	23.550 ± 0.044	0.1167 –

Table 1. Best-fit values obtained for the SALT2 versions of SDSS, Union 2 and SNLS compilations.

In Fig. 2 we show the 68% and 95% confidence contours in the plane (Ω_{m0}, w) for the FwCDM model obtained, via MCMC, using our proposed analysis, for both MLCS2k2 (blue dashed contours) and SALT2 (red solid contours) versions of SDSS compilation. We considered σ_{int} fixed in two particular values $\sigma_{\text{int}} = 0$, in the left panel, and $\sigma_{\text{int}} = 0.15$, in the right panel. We show that σ_{int} is a key parameter to obtain agreement between MLCS2k2 and SALT2 analyses at 68% confidence level.

MLCS2k2

SDSS	Λ CDM	Ω_{m0}	Ω_{k0}	h	σ_{int}
	\mathcal{L}	0.386	0.03	0.6374	0.1406
		± 0.071	± 0.20	± 0.0055	± 0.0073
	χ^2	0.395	0.03	0.6367	0.1917
		± 0.083	± 0.24	± 0.0070	–
	Fw CDM	Ω_{m0}	w	h	σ_{int}
\mathcal{L}	0.418	–1.08	0.6393	0.1406	
	± 0.089	± 0.35	± 0.0068	± 0.0074	
χ^2	0.432	–1.12	0.6392	0.1883	
	± 0.097	± 0.42	± 0.0085	–	

Table 2. Best fit values for the MLCS2k2 version of the SDSS compilation.

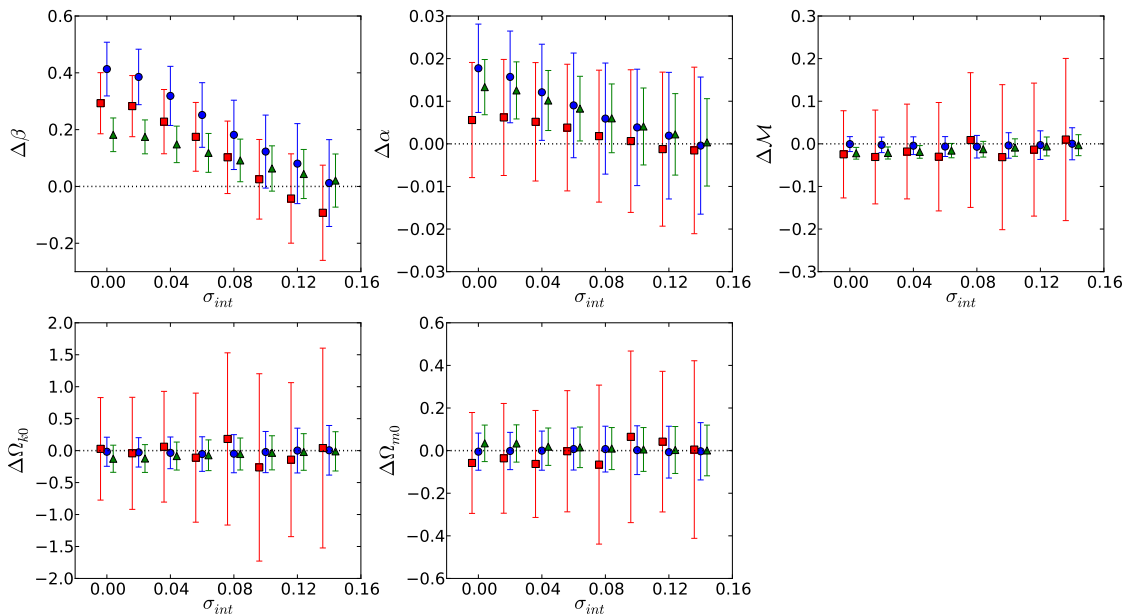


Figure 1. Dependence of SALT2 best-fit parameters discrepancies on σ_{int} for the SDSS (blue circles), Union 2 (green triangles) and SNLS (red squares). $\Delta\Theta_i$ represents the difference between the values obtained through the likelihood and χ^2 analyses. The Λ CDM model was used in this analysis.

5.2 Comparison of model selection

As mentioned previously, imposing that the reduced- χ^2 equals unity, even in an intermediate step, compromises the discrimination of cosmological models, as usually performed by means of information criteria since, imposing this condition, one is assuming that the model is the best, regardless of the actual probability distribution of the model parameters. This inconsistency was also pointed out by [67]. By using the likelihood analysis, one can discriminate models in a consistent way, since it is always driven by the likelihood at all steps.

In order to show the differences between the two approaches, we chose two information

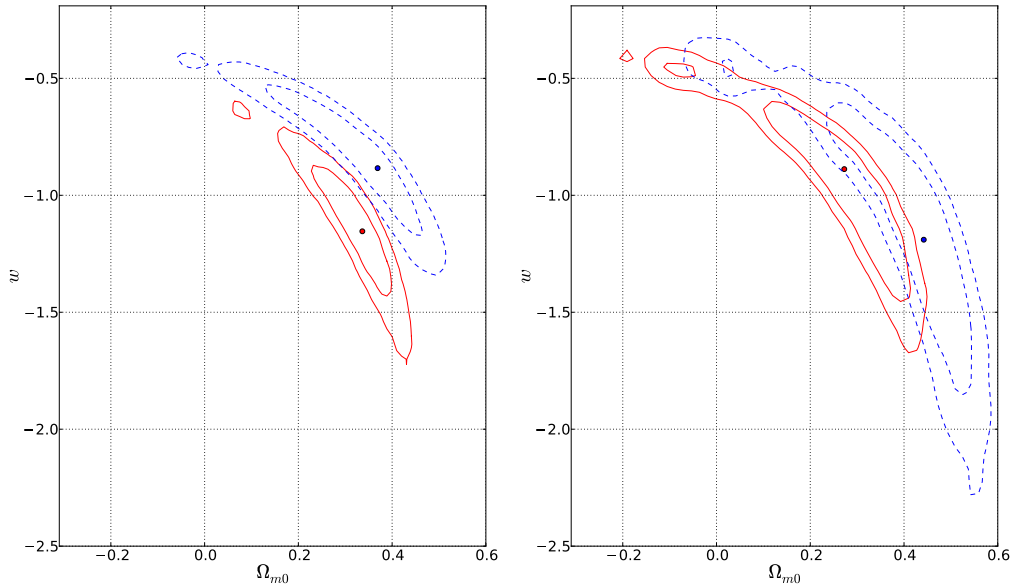


Figure 2. Constraints on FwCDM model parameters from SDSS compilation dataset, considering both MLCS2k2 (blue dashed contours) and SALT2 (red solid contours) versions, using the likelihood analysis. *left panel:* 68% and 95% confidence contours in (Ω_{m0}, w) plane imposing $\sigma_{\text{int}} = 0$. *right panel:* 68% and 95% confidence contours in (Ω_{m0}, w) plane imposing $\sigma_{\text{int}} = 0.15$.

criteria to rank the models [68]. The first one is the Akaike Information Criterion (AIC) [69] which is defined as

$$\text{AIC} = \mathcal{L}_{\min} + 2N_{\text{par}}, \quad (5.5)$$

where N_{par} is the number of independent parameters of the model. The best model is the one which minimizes the AIC. The second one is the Bayesian Information Criterion (BIC) [70] defined as

$$\text{BIC} = \mathcal{L}_{\min} + N_{\text{par}} \ln N, \quad (5.6)$$

where N is, as before, the number of data points (288 for SDSS, 557 for Union2, and 251 for SNLS). It is important to highlight that BIC assumes that the data points are independent and identically distributed.

Although the information criteria are given in terms of the likelihood of the problem under consideration, when using the χ^2 analysis, it is replaced by the minimum χ^2 in Eqs. (5.5) and (5.6), and in any other information criterion definition, equivalently. Here, we are referring to this approach when we mention AIC or BIC. In the likelihood analysis, we use the actual value of \mathcal{L}_{\min} in Eqs. (5.5) and (5.6). Table 3 summarizes the models used in the comparison and the parameters considered free in the fit. The results obtained using AIC and BIC for the χ^2 and likelihood analyses are presented in Tables 4 and 5.

Analyzing the information criteria results, we see from Table 4 that, when using SALT2 output, the χ^2 analysis prefers FDGP for all samples, while the likelihood analysis prefers FDGP for SDSS sample and FACDM for Union2 and SNLS. From Table 5, when using MLCS2k2 output, the χ^2 prefers Λ CDM and the likelihood prefers FACDM. We find that (from Tables 4 and 5), for both analyses, AIC does not provide significant evidence against

model	θ
w CDM	$\Omega_{m0}, \Omega_{k0}, w$
Fw CDM	Ω_{m0}, w
Λ CDM	Ω_{m0}, Ω_{k0}
$F\Lambda$ CDM	Ω_{m0}
FDGP	Ω_{m0}
GCG	Ω_{k0}, A, α_c
FGCG	A, α_c

Table 3. Models considered and their corresponding θ parameter vectors. Flat models are indicated by the “F”.

SALT2

	\mathcal{L}			χ^2		
	Model	Δ AIC	Δ BIC	Model	Δ AIC	Δ BIC
SDSS	FDGP	0.00	0.00	FDGP	0.00	0.00
	$F\Lambda$ CDM	0.02	0.02	$F\Lambda$ CDM	0.11	0.11
	Λ CDM	1.97	5.63	Fw CDM	0.97	4.63
	FGCG	1.98	5.64	FGCG	0.98	4.64
	Fw CDM	1.99	5.65	Λ CDM	1.00	4.66
	w CDM	3.87	11.20	w CDM	2.07	9.39
	GCG	3.91	11.23	GCG	2.12	9.45
Union 2	$F\Lambda$ CDM	0.00	0.00	FDGP	0.00	0.00
	FDGP	0.22	0.22	$F\Lambda$ CDM	0.08	0.08
	Fw CDM	1.96	6.28	Λ CDM	1.15	5.47
	FGCG	1.99	6.31	FGCG	1.22	5.54
	Λ CDM	2.00	6.32	Fw CDM	1.32	5.64
	GCG	3.62	12.27	w CDM	2.10	10.74
	w CDM	3.68	12.32	GCG	2.12	10.76
SNLS	$F\Lambda$ CDM	0.00	0.00	FDGP	0.00	0.00
	FDGP	0.01	0.01	$F\Lambda$ CDM	0.05	0.06
	Fw CDM	1.98	5.51	Fw CDM	1.08	4.60
	FGCG	1.99	5.52	FGCG	1.10	4.62
	Λ CDM	2.00	5.52	Λ CDM	1.11	4.64
	w CDM	3.94	10.99	w CDM	1.95	9.01
	GCG	3.95	11.00	GCG	2.15	9.20

Table 4. Model comparison for the likelihood and χ^2 analyses, both for the SALT2 version of SDSS, Union 2 and SNLS datasets (top, middle and bottom tables, respectively). For all samples, models are ordered from the lowest to the highest Δ AIC values.

any of the chosen models, except for a strong evidence (Δ IC>5) [68] against FDGP in the χ^2 one, via MLCS2k2 output. As concerns BIC, however, the likelihood analysis yields slightly more power of discrimination, giving either a decisive evidence (Δ IC>10) [68] or a strong one against some models, while the χ^2 provides similar evidence only the Union2 SALT2 case.

MLCS2k2

		\mathcal{L}			χ^2		
		Model	ΔAIC	ΔBIC	Model	ΔAIC	ΔBIC
SDSS	ΛCDM	0.00	0.00	ΛCDM	0.00	0.00	
	FDGP	0.11	0.11	GCG	0.81	4.47	
	$w\text{CDM}$	0.86	8.18	$w\text{CDM}$	3.07	6.73	
	$Fw\text{CDM}$	1.97	5.64	FGCG	3.85	3.84	
	ΛCDM	1.99	5.65	ΛCDM	3.94	0.28	
	FGCG	2.00	5.66	$Fw\text{CDM}$	4.33	4.33	
	GCG	3.60	10.92	FDGP	5.10	1.44	

Table 5. Model comparison for the likelihood and χ^2 analyses, both for the MLCS2k2 version of SDSS dataset. Models are ordered from the lowest to the highest ΔAIC values.

5.3 Investigating evolution of the SALT2 parameters α , β , \mathcal{M} and σ_{int} with redshift

We also allow for a possible variation of the parameters α , β , \mathcal{M} and σ_{int} with redshift, in the context of the SALT2 likelihood analysis. In order to perform such an analysis the datasets were divided in redshift bins and the cosmological parameters were fixed in the best-fit values obtained from the global fit, then releasing α , β , \mathcal{M} and σ_{int} to be determined in each bin. This analysis was performed only in the likelihood context. The results are shown in Fig. 3. We found evidence of evolution for α and β , in agreement with [16]; furthermore we also found evidence of evolution for σ_{int} , when using the SDSS compilation dataset, which might support the use of a function of redshift, instead of a constant, for σ_{int} .

6 Conclusions

In this work we scrutinized the statistical analysis, common in the literature on SNe Ia, in which the best fit values for the model parameters are determined by minimizing a traditional χ^2 function, in which the variance is not completely known, but rather depends on the model parameters as well as additional ones. We argued that, in this case, minimizing χ^2 is not formally equivalent to maximizing the likelihood function of the problem, since the normalization of the likelihood, assumed Gaussian, is also a function of the parameters to be determined [cf. Eq. (4.2)]. We proposed to use a consistent, grounded and simple alternative: maximizing the actual probability density of the problem, the likelihood.

We used three of the most recent SNe Ia datasets: the SDSS first year, the Union2 and the SNLS third year compilations, processed by two of the most used light curve fitters in the literature, the MLCS2k2 and the SALT2. MLCS2k2 gives a cosmology-independent estimation of the distance modulus for each SN Ia, with its corresponding variance, which can be directly compared with the model prediction for this quantity. The SALT2 is not a distance estimator, consequently, we can only have an estimate of the distance modulus depending on parameters to be obtained simultaneously with the cosmological ones. In addition, in both analyses, it is common to introduce a residual, unknown, contribution σ_{int} to the variance which is determined by imposing that the reduced χ^2 be unity, when considering the full sample, in the SALT2 case, or only nearby SNe Ia, in the MLCS2k2 case.

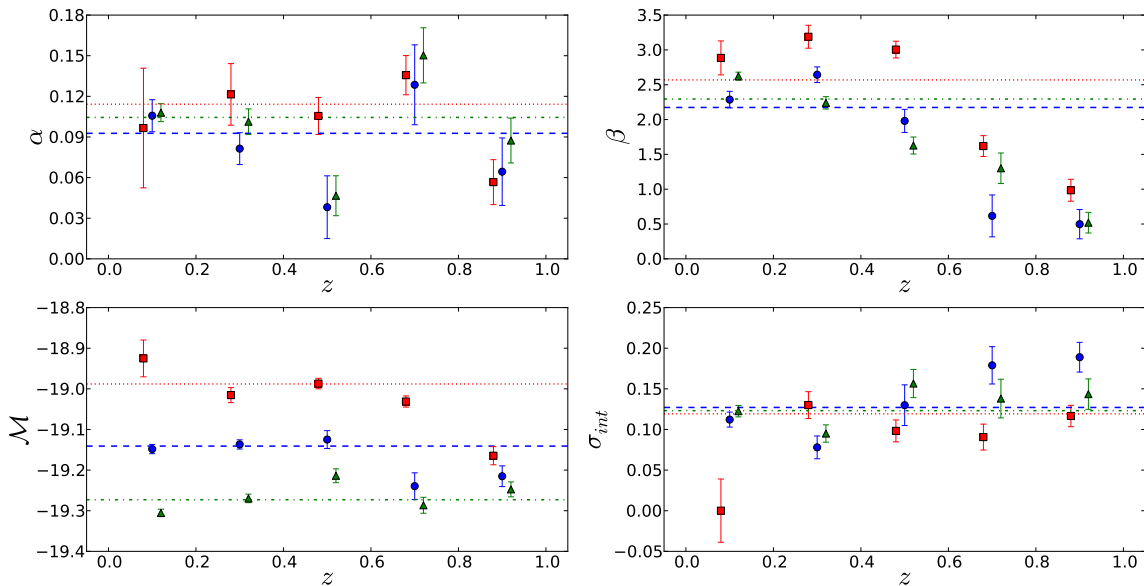


Figure 3. Evolution of SALT2 parameters for the SDSS (blue circles), Union 2 (green triangles) and SNLS (red squares). The dashed, dot-dashed and dotted lines represent the values obtained in the global fit for SDSS, Union 2 and SNLS samples respectively.

The results obtained from the χ^2 analysis were compared with the likelihood one, in which we find the best fit by maximizing the likelihood. For the chosen cosmological models, we showed that there is no significant difference in neither the best fit values nor the 68% confidence intervals, for the present data (cf. Tables 1 and 2).

The role of σ_{int} , in the apparent equivalence between the two approaches, was investigated considering a hypothetical situation in which we know exactly its value and see how the difference between the best fit values of the other parameters, for both analyses, using SALT2 output, changes with the (fixed) value of σ_{int} . We found that the difference for the parameters $\delta = (\alpha, \beta)$ increases for lower σ_{int} such that the results become incompatible at 68% of confidence level for $\sigma_{\text{int}} \lesssim 0.08$ (cf. Fig. 1). This can be considered as an evidence for a possible significant discrepancy between the analyses for future data.

Still while dealing with best-fit parameter and confidence contour estimation, we showed that the use of a non-vanishing σ_{int} is crucial to make the proposed likelihood analyses from the MLCS2k2 and SALT2 output compatible within 95% confidence level (cf. Fig. 2).

The problem of model selection was considered and we investigated the ranking of a set of cosmological models, obtained with the information criteria AIC and BIC, when using both analyses. We found that the classification does depend on the analysis, though marginally (cf. Tables 4 and 5).

We also studied the possible evolution of the SALT2 parameters α , β and \mathcal{M} with the redshift, splitting the samples in redshift bins and performing the fit separately for each one. In this situation, we found evidence of evolution in agreement with [16] (cf. Fig. 3).

While this paper was in preparation two articles addressing the issue of using χ^2 with unknown variances appeared in the arXiv. The first one [71] focused on the question of the determination of σ_{int} , using simulated data as MLCS2k2 output, which prevented the

investigation of the problem with SALT2. The second one [72] studied the SALT2 case and presented essentially the same criticisms that we showed in this work. It proposed as alternative a sophisticated Bayesian analysis based on posterior probability density functions instead of our simpler, more direct proposal based on the likelihood.

We conclude that, although for present data and for a few cosmological models there is no significant difference in the best fit values between the analyses examined, it is dangerous to postulate that such apparent equivalence will remain for every model and for future data. We strongly recommend the use of the likelihood framework for whatever SNe Ia analysis since it is a consistent, well grounded and numerically efficient approach to the problem.

References

- [1] A. G. Riess *et alii*, “Observational evidence from supernovae for an accelerating universe and a cosmological constant”, *Astron. J.* **116**, 1009 (1998) [astro-ph/9805201].
- [2] S. Perlmutter *et alii*, “Measurements of Ω and Λ from 42 high-redshift supernovae”, *Astrophys. J.* **517**, 565 (1999) [astro-ph/9812133].
- [3] E. Hubble, “A relation between distance and radial velocity among extra-galactic nebulae”, *Proc. Nat. Acad. Sci. USA* **15**, 168 (1929).
- [4] E. Komatsu *et alii*, “Seven-year *Wilkinson Microwave Anisotropy Probe (WMAP)* observations: cosmological interpretation”, *Astrophys. J. Suppl.* **192**, 18 (2011) [arXiv:1001.4538].
- [5] D. J. Eisenstein *et alii*, “Detection of the baryon acoustic peak in the large-scale correlation function of SDSS luminous red galaxies”, *Astrophys. J.* **633**, 560 (2005) [astro-ph/0501171].
- [6] W. J. Percival *et alii*, “Baryon acoustic oscillations in the Sloan Digital Sky Survey Data Release 7 galaxy sample”, *Mon. Not. Roy. Astron. Soc.* **401**, 2148 (2010) [arXiv:0907.1660].
- [7] A. Vikhlinin *et alii*, “*Chandra* cluster cosmology project III: cosmological parameter constraints”, *Astrophys. J.* **692**, 1060 (2009) [arXiv:0812.2720].
- [8] A. Mantz *et alii*, “The Observed Growth of Massive Galaxy Clusters I: Statistical Methods and Cosmological Constraints”, *Mon. Not. Roy. Astron. Soc.* **406**, 1759 (2010) [arXiv:0909.3098].
- [9] M. M. Phillips, “The absolute magnitudes of type Ia supernovae”, *Astrophys. J.* **413**, L105 (1993).
- [10] T. E. Vaughan *et alii*, “The blue and visual magnitude distributions of type Ia supernovae”, *Astrophys. J.* **439**, 558 (1995).
- [11] M. Hamuy *et alii*, “The absolute luminosities of the Calán/Tololo type Ia supernovae”, *Astron. J.* **112**, 2391 (1996) [astro-ph/9609059].
- [12] G. Contardo, B. Leibundgut, and W. D. Vacca, “Epochs of maximum light and bolometric light curves of type Ia supernovae”, *Astron. Astrophys.* **359**, 876 (2000) [astro-ph/0005507].
- [13] W. M. Wood-Vasey *et alii*, “Observational constraints on the nature of dark energy: first cosmological results from the ESSENCE supernova survey”, *Astrophys. J.* **666**, 694 (2007) [astro-ph/0701041] [ESSENCE].
- [14] M. Kowalski *et alii*, “Improved cosmological constraints from new, old, and combined supernova data sets”, *Astrophys. J.* **686**, 749 (2008) [arXiv:0804.4142] [Union].
- [15] M. Hicken *et alii*, “Improved dark energy constraints from ~ 100 new CfA supernova type Ia light curves”, *Astrophys. J.* **700**, 1097 (2009) [arXiv:0901.4804] [Constitution].
- [16] R. Kessler *et alii*, “First-year Sloan Digital Sky Survey-II supernova results: Hubble diagram and cosmological parameters”, *Astrophys. J. Suppl.* **185**, 32 (2009) [arXiv:0908.4274] [SDSS].

- [17] R. Amanullah *et alii*, “Spectra and *Hubble Space Telescope* light curves of six type Ia supernovae at $0.511 < z < 1.12$ and the Union2 compilation”, *Astrophys. J.* **716**, 712 (2010) [arXiv:1004.1711] [Union2].
- [18] A. Conley *et alii*, “Supernova constraints and systematic uncertainties from the first three years of the Supernova Legacy Survey”, *Astrophys. J. Suppl.* **192**, 1 (2011) [arXiv:1104.1443] [SNLS].
- [19] <http://pan-starrs.ifa.hawaii.edu/>.
- [20] <http://www.darkenergysurvey.org/>.
- [21] <http://www.lsst.org/>.
- [22] B. Dilday *et alii*, “Measurements of the rate of type Ia supernovae at redshift $\lesssim 0.3$ from Sloan Digital Sky Survey II survey”, *Astrophys. J.* **713**, 1026 (2010) [arXiv:1001.4995].
- [23] B. T. Hayden *et alii*, “Single or double degenerate progenitors? Searching for shock emission in the SDSS-II type Ia supernovae”, *Astrophys. J.* **722**, 1691 (2010) [arXiv:1008.4797].
- [24] D. Maoz, “Type Ia supernovae: new clues to their progenitors from the delay time distribution” [arXiv:1011.1014].
- [25] M. Sullivan *et alii*, “The dependence of type Ia supernovae luminosities on their host galaxies”, *Mon. Not. R. Astron. Soc.* **406**, 782 (2010) [arXiv:1003.5119].
- [26] H. Lampeitl *et alii*, “The effect of host galaxies on type Ia supernovae in the SDSS-II supernova survey”, *Astrophys. J.* **722**, 566 (2010) [arXiv:1005.4687].
- [27] W. Hillebrandt and J. C. Niemeyer, “Type Ia supernova explosion models”, *Annu. Rev. Astron. Astrophys.* **38**, 191 (2000) [astro-ph/0203369].
- [28] S. Nobili *et alii*, “Constraining dust and color variations of high- z SNe using NICMOS on the *Hubble Space Telescope*”, *Astrophys. J.* **700**, 1415 (2009) [arXiv:0906.4318].
- [29] N. Yasuda and M. Fukugita, “Luminosity functions of type Ia supernovae and their host galaxies from the Sloan Digital Sky Survey”, *Astron. J.* **139**, 39 (2010) [arXiv:0905.4125].
- [30] P. Nugent, A. Kim and S. Perlmutter, “K-corrections and extinction corrections for type Ia supernovae”, *Pub. Astron. Soc. Pacific* **114**, 803 (2002) [astro-ph/0205351].
- [31] E. Y. Hsiao *et alii*, “K-corrections and spectral templates of type Ia supernovae”, *astrophys. J.* **663**, 1187 (2007) [astro-ph/0703529].
- [32] L. Faccioli *et alii*, “Reducing zero-point systematics in dark energy supernova experiments” [arXiv:1004.3511].
- [33] L. Hui and P. B. Greene, “Correlated fluctuations in luminosity distance and the importance of peculiar motion in supernova surveys”, *Phys. Rev D* **73**, 123526 (2006) [astro-ph/0512159].
- [34] T. M. Davis *et alii*, “The effect of peculiar velocities on supernova cosmology” [arXiv:1012.2912].
- [35] Y. Wang, “Observational signatures of the weak lensing magnification of supernovae”, *J. Cosmol. Astropart. Phys.* **03** (2005), 005 [astro-ph/0406635].
- [36] T. Kronborg *et alii*, “Gravitational lensing in the Supernova Legacy Survey (SNLS)” [arXiv:1002.1249].
- [37] D. A. Howell, “A review of type Ia supernovae as stellar endpoints and cosmological tools” [arXiv:1011.0441].
- [38] R. P. Kirshner, “Foundations of supernova cosmology” in “Dark energy— observational and theoretical approaches”, edited by Pilar Ruiz-Lapuente, Cambridge University Press (2010) [arXiv:0910.0257].
- [39] A. Goobar and B. Leibundgut, “Supernova cosmology: legacy and future”, [arXiv:1102.1431].

- [40] A. G. Riess, W. H. Press and R. P. Kirshner, “Using type Ia supernova light curve shapes to measure the Hubble constant”, *Astrophys. J.* **438**, L17 (1995).
- [41] S. Jha, A. G. Riess and R. P. Kirshner, “Improved distances to type Ia supernovae with multicolor light-curve shapes: MLCS2k2”, *Astrophys. J.* **659**, 122 (2007) [astro-ph/0612666].
- [42] S. Perlmutter *et alii*, “Measurements of the cosmological parameters Ω and Λ from the first seven supernovae at $z \geq 0.35$ ”, *Astrophys. J.* **483**, 565 (1997) [astro-ph/9608192].
- [43] G. Goldhaber *et alii*, “Timescale stretch parameterization of type Ia supernova B -band light curves”, *Astrophys. J.* **558**, 359 (2001) [astro-ph/0104382].
- [44] M. M. Phillips *et alii*, “The redenning-free decline rate versus luminosity relationship for type Ia supernovae” *Astron. J.* **118**, 1766 (1999) [astro-ph/9907052].
- [45] J. L. Prieto, A. Rest and N. B. Suntzeff, “A new method to calibrate the magnitudes of type Ia supernovae at maximum light”, *Astrophys. J.* **647**, 501 (2006) [astro-ph/0603407].
- [46] R. Tripp and D. Branch, “Determination of the Hubble constant using a two-parameter luminosity correction for type Ia supernovae”, *Astrophys. J.* **525**, 209 (1999) [astro-ph/9904347].
- [47] J. L. Tonry *et alii*, “Cosmological results from high- z supernovae”, *Astrophys. J.* **594**, 1 (2003) [astro-ph/0305008].
- [48] S. A. Rodney and J. L. Tonry, “Fuzzy supernova templates. I. Classification”, *Astrophys. J.* **707**, 1064 (2009) [arXiv:0910.3702].
- [49] L. Wang *et alii*, “Multicolor light curves of type Ia supernovae on the color-magnitude diagram: a novel step toward more precise distance and extinction estimates”, *Astrophys. J.* **590**, 944 (2003) [astro-ph/0302341].
- [50] X. Wang *et alii*, “A novel color parameter as a luminosity calibrator for type Ia supernovae”, *Astrophys. J.* **620**, L87 (2005) [astro-ph/0501565].
- [51] B. Reindl *et alii*, “Reddening, absorption, and decline rate corrections for a complete sample of type Ia supernovae leading to a fully corrected Hubble diagram to $v < 30,000 \text{ km s}^{-1}$ ”, *Astrophys. J.* **624**, 532 (2005) [astro-ph/0501664].
- [52] J. Guy *et alii*, “SALT: a spectral adaptive light curve template for type Ia supernovae”, *Astron. Astrophys.* **443**, 781 (2005) [astro-ph/0506583].
- [53] J. Guy *et alii*, “SALT2: using distant supernovae to improve the use of type Ia supernovae as distance indicators” ,*Astron. Astrophys.* **466**, 11 (2007) [astro-ph/0701828].
- [54] A. Conley *et alii*, “SiFTO: an empirical method for fitting SN Ia light curves”, *Astrophys. J.* **681**, 482 (2008) [arXiv:0803.3441].
- [55] K. S. Mandel *et alii*, “Type Ia supernova light-curve inference: hierarchical Bayesian analysis in the near-infrared”, *Astrophys. J.* **704** 629 (2009) [arXiv:0908.0536].
- [56] S. A. Rodney and J. L. Tonry, “Fuzzy supernova templates. II. Parameter estimation”, *Astrophys. J.* **715**, 323 (2010) [arXiv:1003.5724].
- [57] C. R. Burns *et alii*, “The Carnegie Supernova Project: Light-curve fitting with SNooPy”, *Astron. J.* **141**, 19 (2011) [arXiv:1010.4040].
- [58] A. G. Riess, W. H. Press and R. P. Kirshner, “A precise distance indicator: type Ia supernova multicolor light-curve shapes”, *Astrophys. J.* **473**, 88 (1996) [astro-ph/9604143].
- [59] P. Astier *et alii*, “The Supernova Legacy Survey: measurement of Ω_M , Ω_Λ and w from the first year data set”, *Astron. Astrophys.* **447**, 31 (2006) [astro-ph/0510447].
- [60] G. Dvali, G. Gabadadze and M. Porrati, “A Comment on brane bending and ghosts in theories with infinite extra dimensions”, *Phys. Lett. B* **484**, 129 (2000) [hep-th/0003054].

- [61] A. Yu. Kamenshchik, U. Moschella and V. Pasquier, “An alternative to quintessence”, *Phys. Lett. B* **511**, 265 (2001) [gr-qc/0103004].
- [62] N. Bilic, G. B. Tupper and R. D. Viollier, “Unification of dark matter and dark energy: the inhomogeneous Chaplygin gas”, *Phys. Lett. B* **535**, 17 (2002) [astro-ph/0111325].
- [63] M. C. Bento, O. Bertolami and A. A. Sen, “Generalized Chaplygin gas, accelerated expansion and dark energy-matter unification”, *Phys. Rev. D* **66**, 043507 (2002) [gr-qc/0202064].
- [64] M. Makler, S. Q. de Oliveira and I. Waga, “Constraints on the generalized Chaplygin gas from supernovae observations”, *Phys. Lett. B* **555**, 1 (2003) [astro-ph/0209486].
- [65] F. James and M. Roos, “Minuit: a system for function minimization and analysis of the parameter errors and correlations”, *Comput. Phys. Commun.*, **10**, 343 (1975).
- [66] I. Antcheva *et alii*, “ROOT: a C++ framework for petabyte data storage, statistical analysis and visualization”, *Comput. Phys. Commun.*, **180**, 2499 (2009).
- [67] R. G. Vishwakarma and J. V. Narlikar, “A critique of supernova data analysis in cosmology”, *Research Astron. Astrophys.* **10**, 1195 (2010) [arXiv:1010.5272].
- [68] A. R. Liddle, “Information criteria for astrophysical model selection”, *Mon. Not. Roy. Astron. Soc.* **377**, L74 (2007) [astro-ph/070113].
- [69] H. Akaike, “A new look at the statistical model identification”, *IEEE Trans. Automat. Control* **19**, 716 (1974).
- [70] G. E. Schwarz, “Estimating the dimension of a model”, *Ann. Statist.* **6**, 461 (1978).
- [71] A. G. Kim, “Type Ia supernova intrinsic magnitude dispersion and the fitting of cosmological parameters”, [arXiv:1101.3513].
- [72] M. C. March *et alii*, “Improved constraints on cosmological parameters from SNIa data” [arXiv:1102.3237].